**<u>Figure S1</u>:** TEM and SEM images of unmodified and H-Lys(Boc)-OH modified SWCNTs. Note, the length of a 50nm diameter bundle of SWCNTs in the right TEM image does not reflect the length of any individual tube. White dots on this TEM are grid imperfections allowing blanching from transmission of electron beams.

(**below**) TEM image of unmodified, bundled SWCNTs prepared by dispersing tubes in DMF then drying a dilute sample on a carbon coated TEM grid. The bundles are similar in girth to those observed by Maruyama in *Chemical Physics Letters*, *Volume 360, Issues 3–4*, *10 July 2002*, *Pages 229-234, Figure 2A*

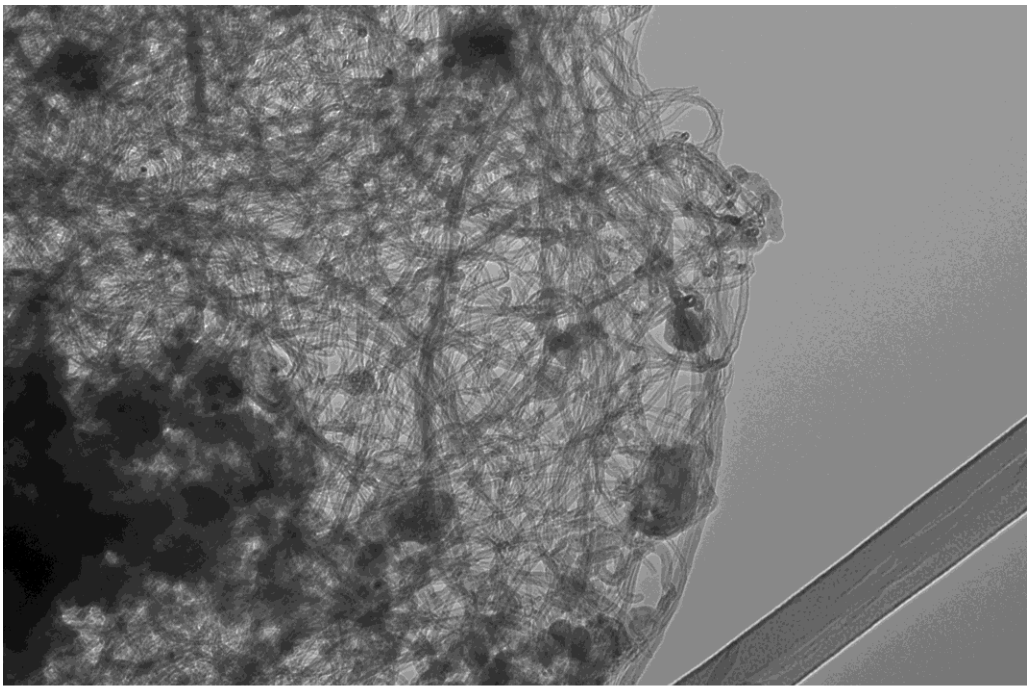


(**left**) TEM image of soluble, functionalized SWCNT-Lys-BOC made by diluting and drying very low concentration, soluble SWCNT-Lys-BOC on a carbon coated TEM grid in distilled water. Bar is 500nm. Overcast circles are grid imperfections. **(right)** SEM image acquired after lyophilizing SWCNT-Lys-BOC into a pellet which was imaged directly

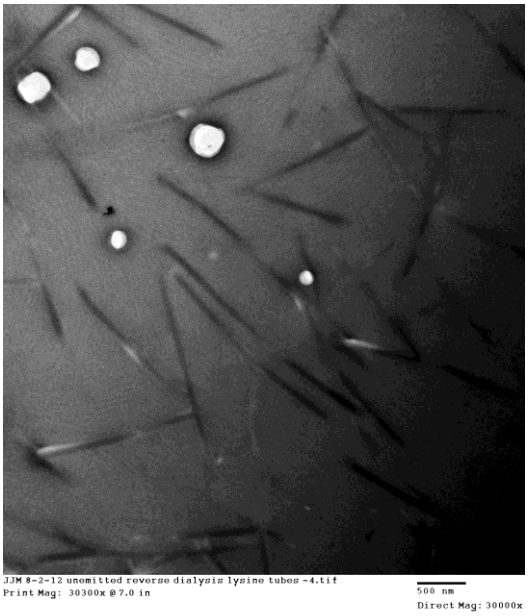


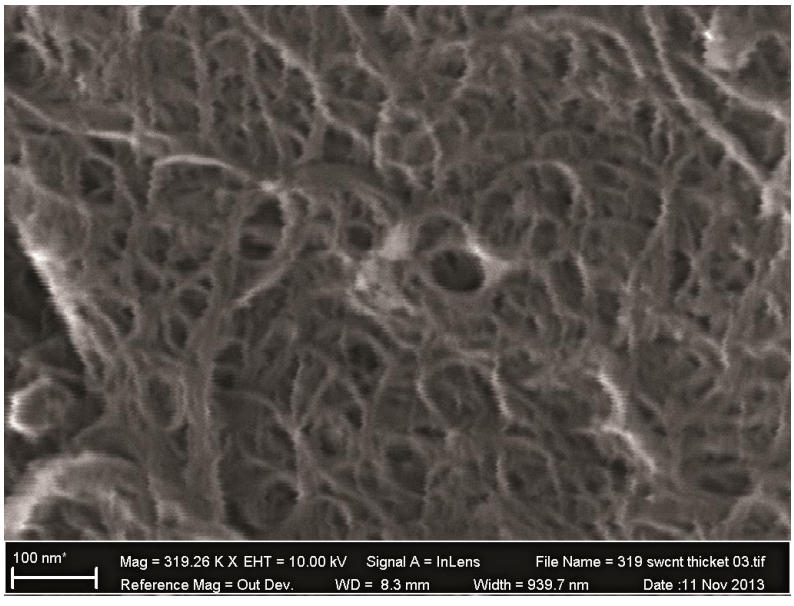

**Figure S2:** Of note in both figures, solvated or not, the bundled nanotubes are large enough to be contained by a 10,000 Molecular Weight Cut-Off membrane. A) Photograph of water soluble, lysine modified SWCNTs undergoing dialysis in a 10,000 MWCO Slidalyzer Dialysis Cassette at pH 7. B) The same sample after adjustment to pH 12. Precipitated SWCNT shown as black granular material.

**A: Solvated, lysine modified SWCNTs (2) at pH 7** **B: Crashed-out, lysine modified SWNTs (2) at pH 12**

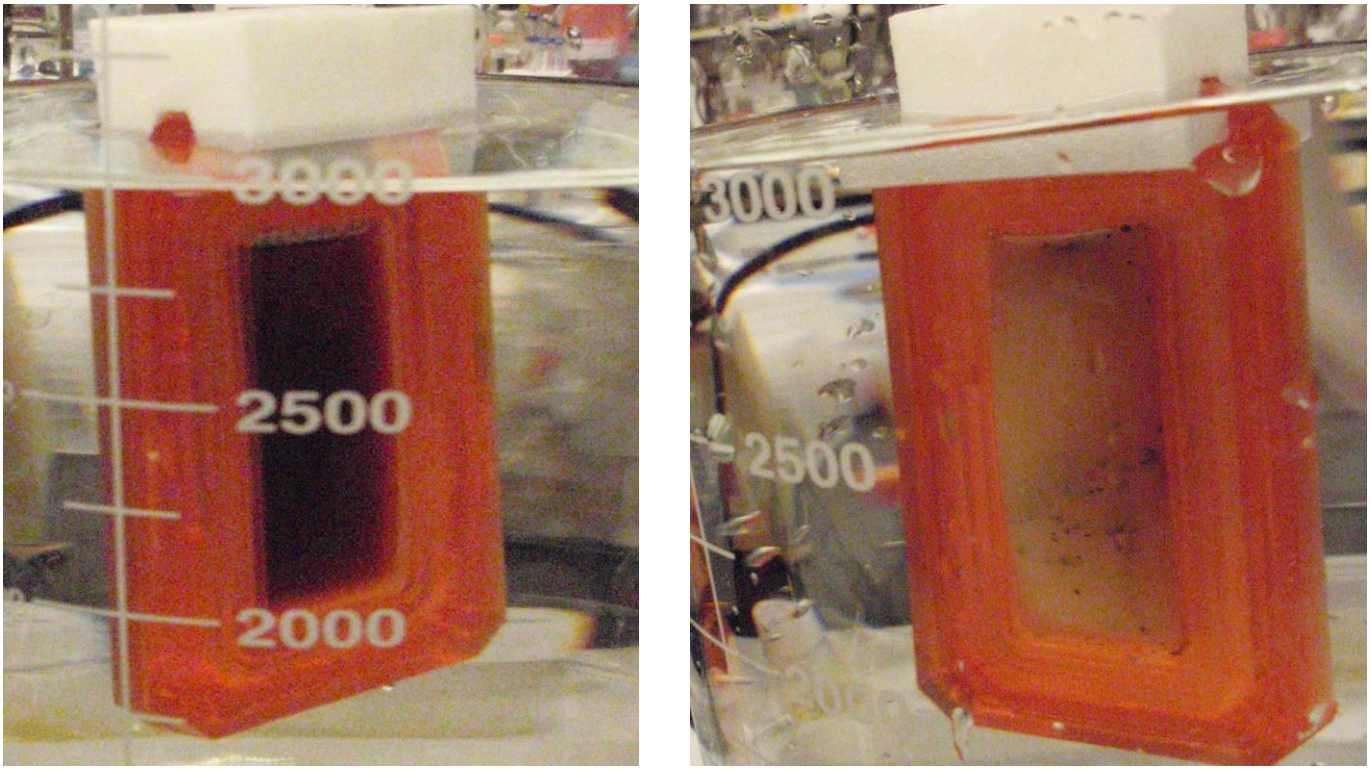


**Figure S3:** Concentration curve derivation from 600nm absorption and HPLC trace of SWCNT-Lys-$NH_2$

**Figure S3*A*:** UV/Vis Absorption Spectrum of (**1**) showing characteristic SWCNT Absorbance slope

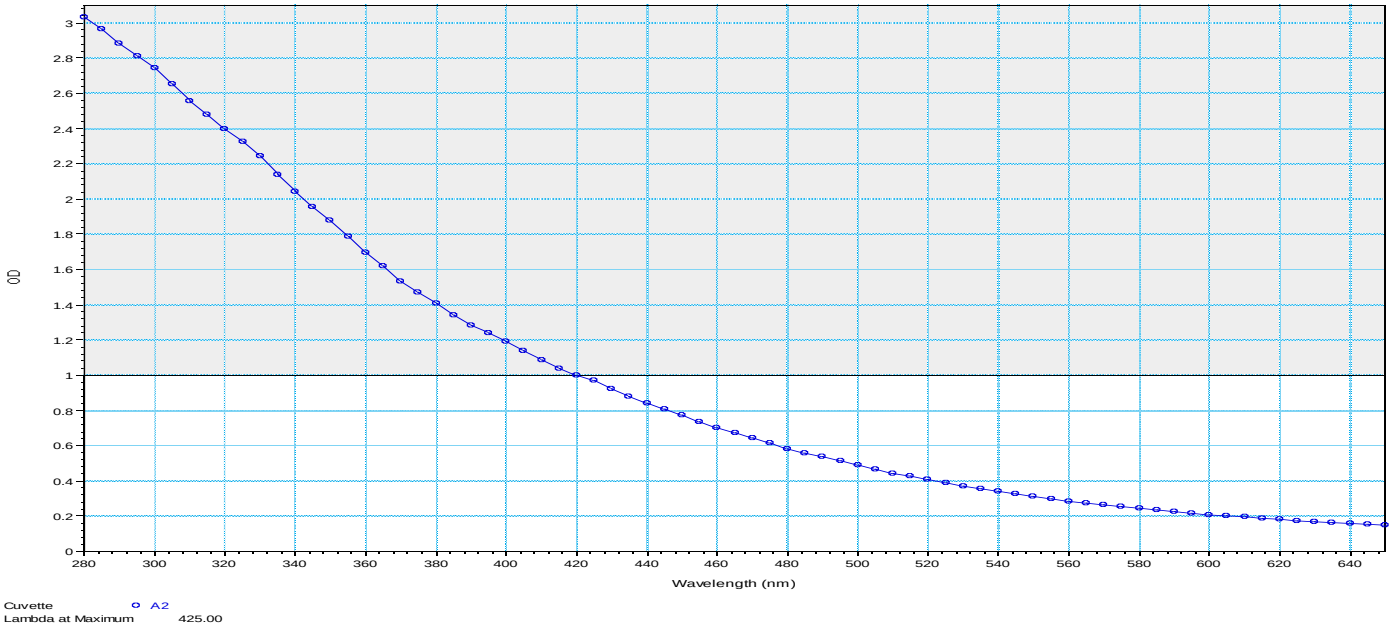

**Figure *S3B*:** UV/Vis Absorption Spectrum of SWCNT-Lys-$NH_2$,(**2**) showing characteristic SWCNT Absorbance slope

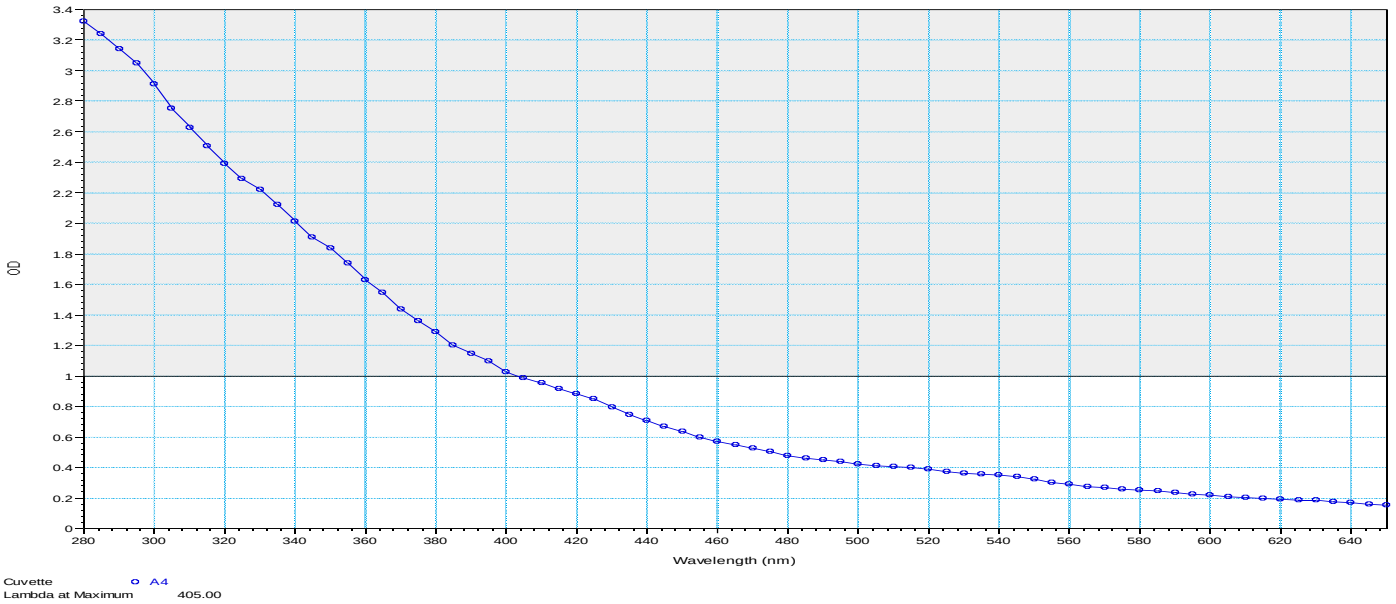


**Figure *S3C*:** SWCNT-Lys-$NH_2$,(**2**) 600nm absorbance versus concentration curve with derived equation.

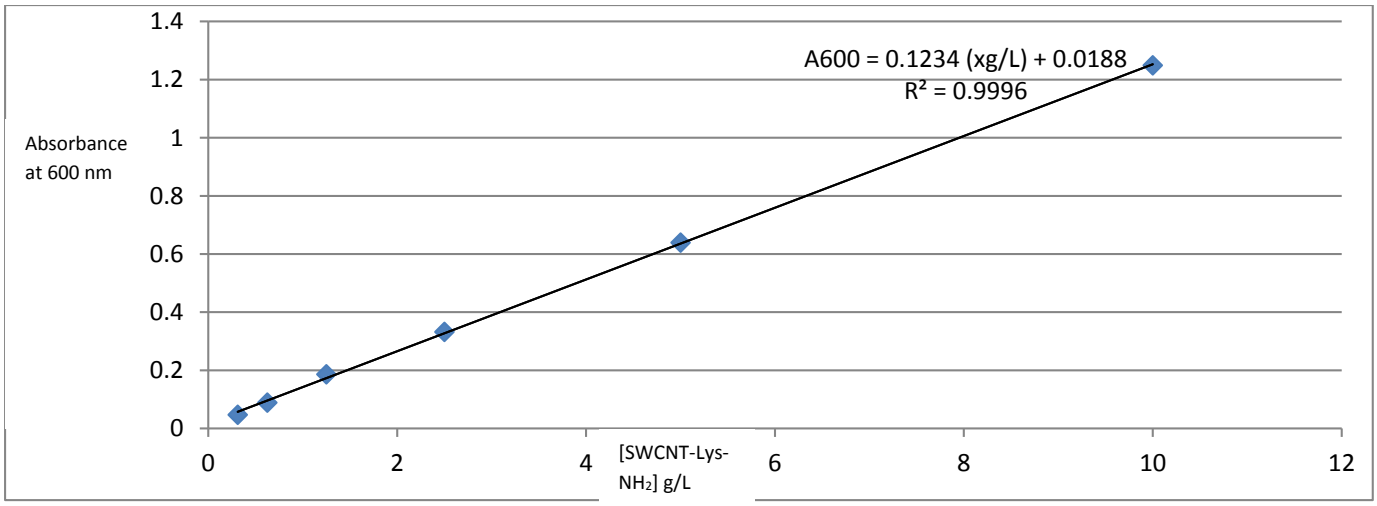


**Figure *S3D*:** SWCNT-Lys-$NH_2$,(**2**) C18 HPLC trace showing single, broad peak in 20-100% gradient of acetonitrile over 50 minutes. This also corroborates the signature slope of modified CNT, and modification enhancements 230-260.

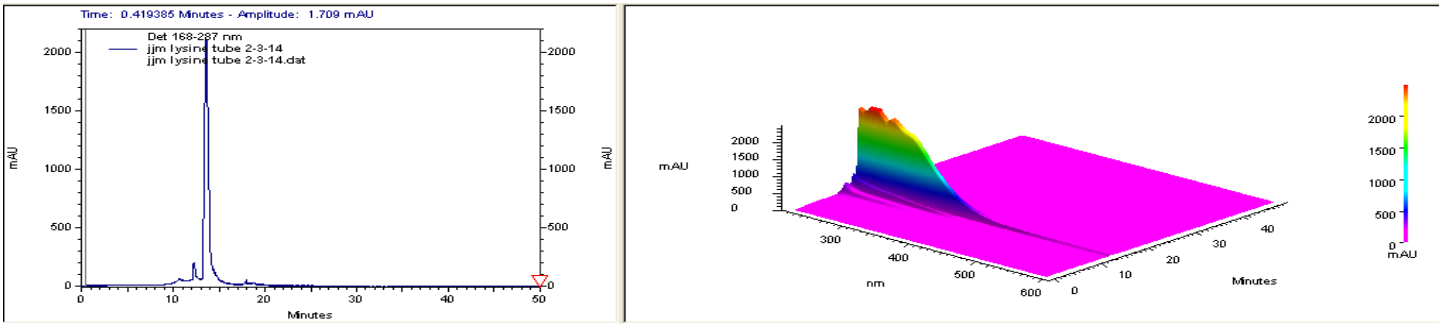

**Figure S4:** Kaiser/Sarin assay and calculation of degree of amine modification

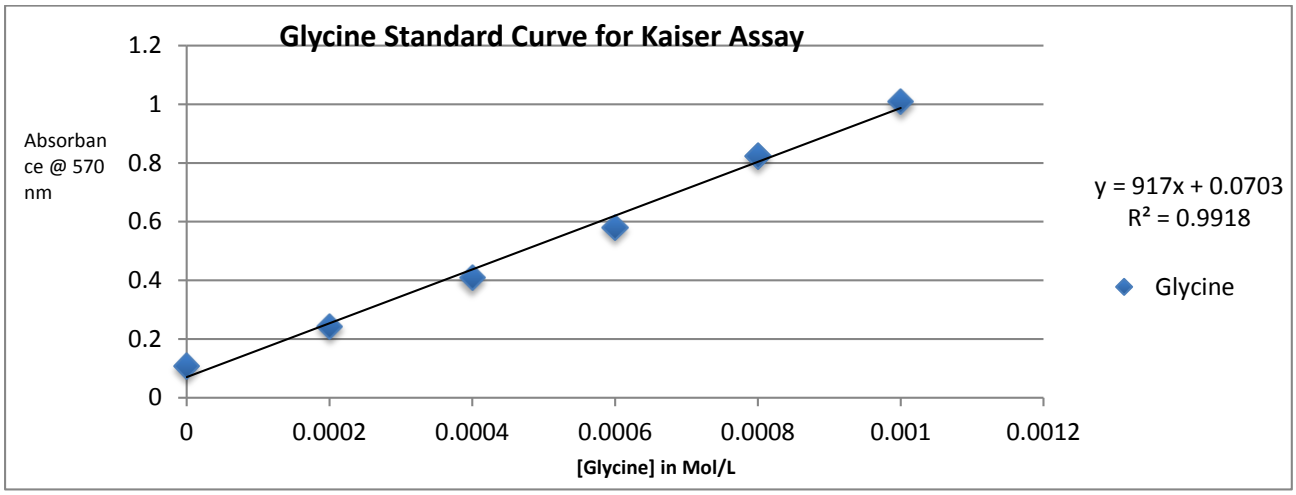


Derived Amine to Absorbance Equation:

A570 = [Molarity of Amines] * 917 + 0.0703

H-Lys(Boc)-OH Generated Product (**2**):

[Concentration of Analyte] = 0.9 g/L (massed and diluted)

A570 = 0.635

[NH2] = 6.16E-4 M

[Carbon] = 0.9 g/L / (12 g /mol) = 0.075 M

→ **1 Amine / 121.8 Carbons**

Prato Reaction Product (**1**):

[Concentration of Analyte] = 0.68 g/L

A570 = 0.375

[NH2] = 3.32E-4 M

[Carbon] = 0.68 g/L / (12 g/mol) = 0.057M

→ **1 Amine / 171.7 Carbons**

Derived Ratio:

170.1/121.8 = 1.41

This analysis was completed twice on separately prepared samples, the second analysis yielding a similar ratio of 1.39.

One possible explanation for the increased functionalization is that the non-polar, carbon lysine side-chain abstains from stabilizing interactions with the ylide during the reaction as a more polar, PEGylated adduct might. Another possible explanation is that without an additional hyperconjugating alkanyl adduct to the ylide nitrogen as seen in the Prato Reaction, the ylide in this reaction would be less stabilized and more reactive. A third, or contributing possibility is that unreacted fullerenes are more quickly exposed to reagents as the more DMF-soluble product on the surface of visible clusters is expediently removed into solution.

**Figure S5:** Solid state FTIR spectra of: **A)** L-lysine. **B)** H-Lys(Boc)-OH (Starting Material.) **C)** Modified SWCNTs. **D)** Modified C60. **E)** *Unpurified* Sigma Aldrich SWCNTs as provided. **F)** *Unpurified* Sigma Aldrich C60 as provided.

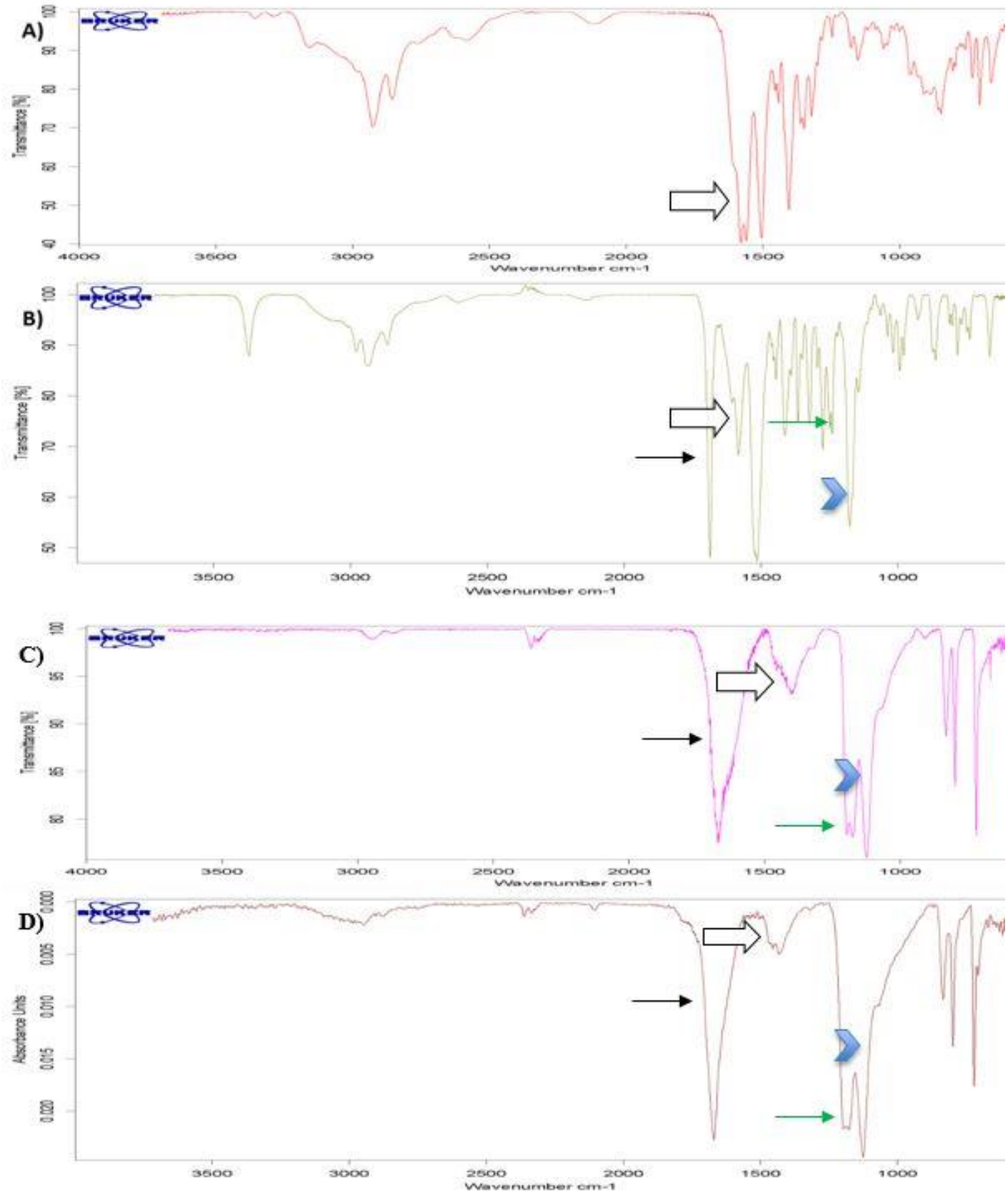

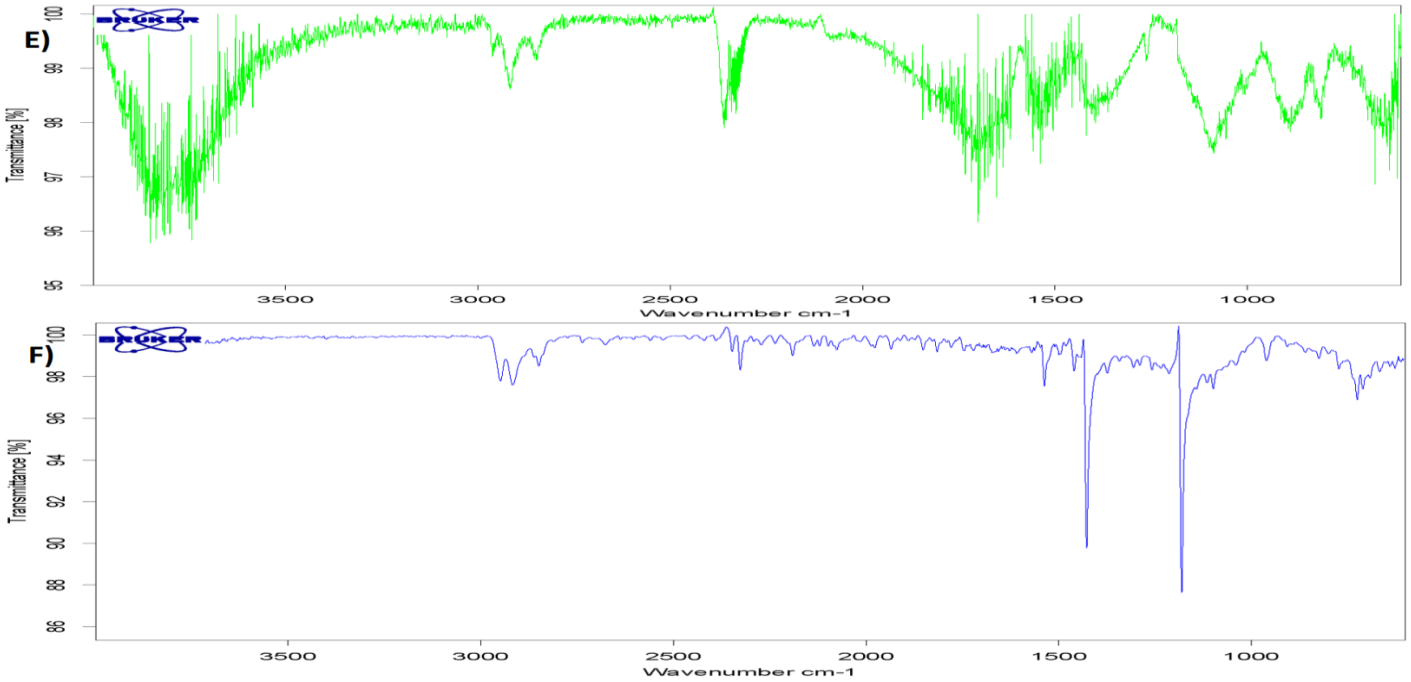


**A)** Shows a characteristic side chain amine N-H wag triad of peaks around 700 $cm^{-1}$. At 1400 $cm^{-1}$ there is an N-H bend from the amino-acid amine (no longer present in (C)), and three peaks at 1500-1600 $cm^{-1}$ representing the N-H bends from the primary side chain amine and the acid carbonyl which is low in energy because it is deprotonated with resonance stabilization. Just below 3000 $cm^{-1}$ are $SP^3$ C-H stretches. The shelf beneath them extending to 3400 $cm^{-1}$ encompasses the primary N-H and acid O-H stretches.

**B)** Very Similar to (A) with a new identifying carbonyl at 1650 $cm^{-1}$ marked by the black arrow representing the BOC carbonyl and more C-O and C-N between 1000 and 1300 $cm^{-1}$. The side chain amine N-H bends mentioned in (A) are recessed since with the BOC group, only one remains from the two on unmodified lysine.

**C)** The strong acid carbonyl peak above 1500 $cm^{-1}$ is gone with the reaction decarboxylation leaving only broadened N-H bends from the triad. The slight energy shift of the triad of peaks marked by the block arrow showing a different chemical environment is supportive of functionalization. At 1650 $cm^{-1}$ the strong carbonyl peak is still present giving convincing evidence that the BOC protecting group is still attached and broadened by underlying C=C stretches The characteristic side chain amine N-H wag triad of the lysine adduct arises around 700 $cm^{-1}$, correlating directly with the spectrum of the amino acid (A). Around 1200 $cm^{-1}$ are the bend of the primary amine, C-O stretches and C-N stretches first seen in B), and at the same level of transmittance as in B). These are marked by a blue chevron and a green arrow. Just below 3000 $cm^{-1}$ are the $SP^3$ C-H stretches of the adduct. These should not be attributed to those peaks shown in (E) as peaks from (E) are attributed to the presence of amorphous carbon species cleared in purifications. The broadness and the ruffles in the BOC carbonyl and the N-H bend at 1400 $cm^{-1}$ are the low intensity jagged peaks of the SWCNT seen at those wavelengths in (E)

**D)** C60 adducted with BOC-protected lysine (BOC not removed). Very similar to (C).

**E)** Depicts significant C=C peaks at 1700 $cm^{-1}$ and 1535 $cm^{-1}$ with a wide variety of discrete energy levels as well as residual CO2 at 2400 $cm^{-1}$, and amorphous carbon impurities seen in the relatively large amount of $SP^3$ C-H stretches.

These $SP^3$ C-H stretches just below 3000 $cm^{-1}$ as well as the shelf below 1200 $cm^{-1}$ are reduced by removal of amorphous carbon and tubes below 25nm in length respectively.[1]

**F)** Two discrete C=C stretches are seen between 1500 $cm^{-1}$ and 1000 $cm^{-1}$ that accord with literature. Far IR shelf at 650 $cm^{-1}$ is representative of fullerenes with size smaller than 25 nanometers on a breathing axis; it is also a sharper peak than seen with the SWCNTs because C60 is of a discrete size. It should be noted that the literature suggests two identifying fingerprint peaks below the end-range of this FTIR instrument (600 $cm^{-1}$). Again, $SP^3$ C-H stretches were consistently present *out of the bottle* and are believed to be amorphous carbon in unpurified starting material.

**Figure S6:** NMR Spectra and Analyses

**Figure S6A*:*** Starting H-Lys(Boc)-OH H-NMR (δ in ppm) in $D_2O$

H-NMR: δ Multiplet=1.44;  δ Singlet=1.47; δ Pentet=1.56; δ Multiplet=1.90; δ triplet=3.12; δ Triplet=1.56; δ Triplet=1.76

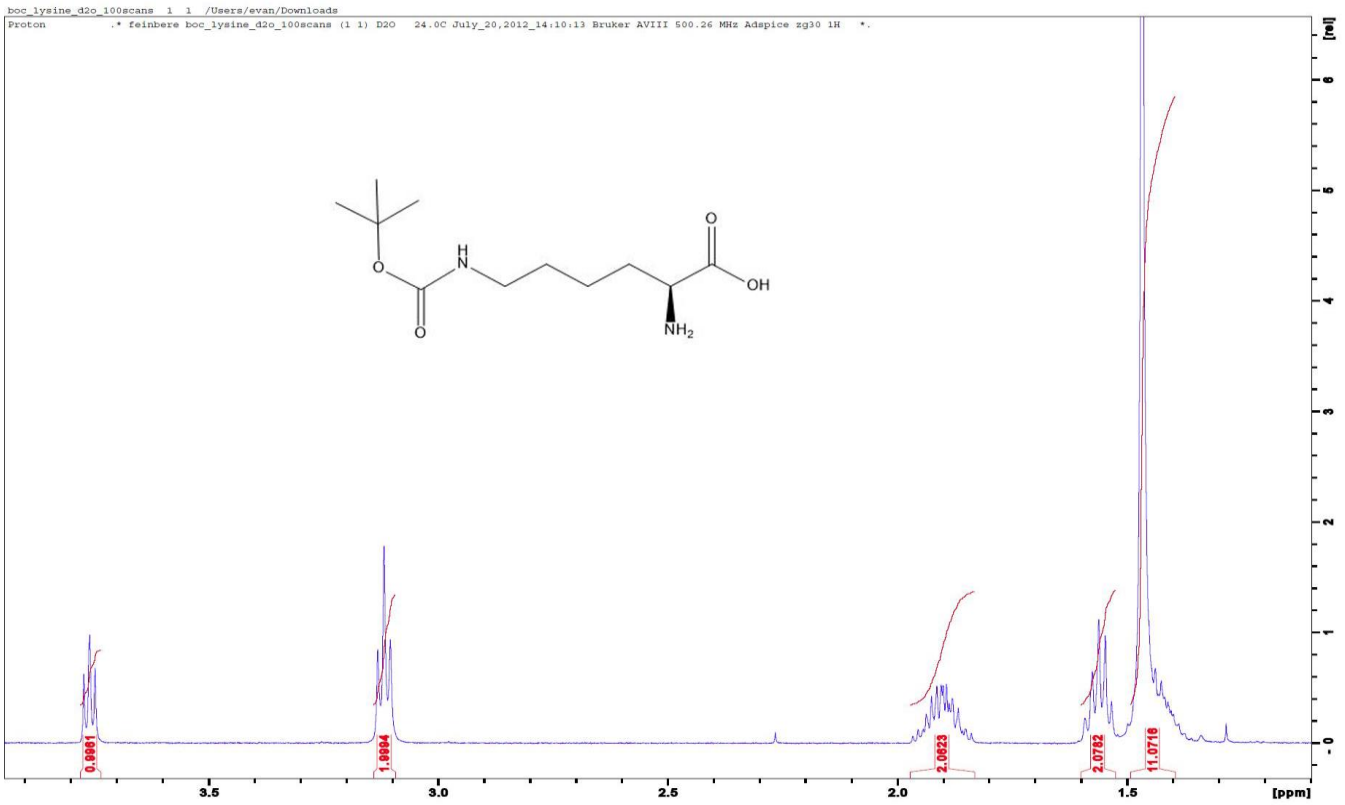


**Figure S6B*:*** Starting H-Lys(Boc)-OH C13-NMR (δ in ppm) in $D_2O$: δ = 21.59;  δ = 27.61; δ = 28.55; δ = 30.06; δ = 39.51; δ = 54.51; δ = 80.83; δ = 158.33; δ = 174.76.  Two carbonyl peaks are seen downfield of 150ppm

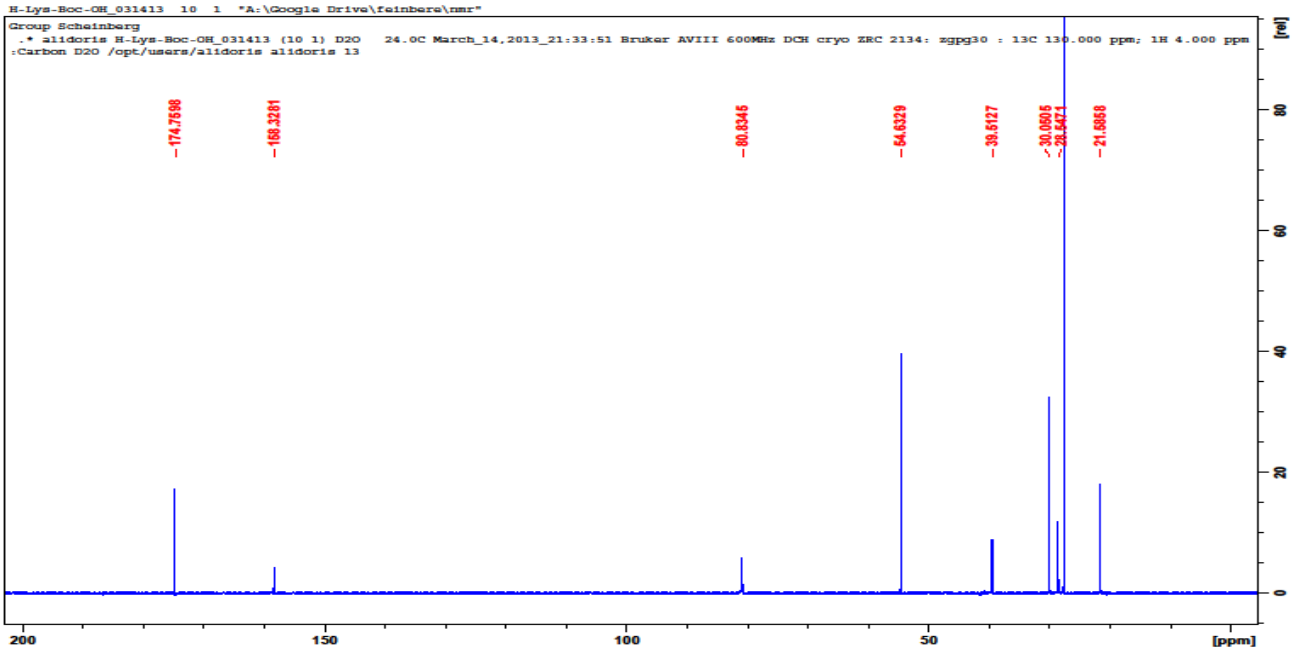

**Figure S6C [Three different zooms of a single spectrum i, ii, iii]**: BOC-protected pyrrolidine adduct on C60 H-NMR (δ in ppm) in $D_2O$

Lysine modified C60 fullerenes were moderately soluble in $D_2O$, slightly soluble in deuterated methanol, sparingly soluble in deuterated acetonitrile, and insoluble in deuterated chloroform, benzene and DMSO. NMR spectra of SWCNT were similar, but less resolved.

We ascribe upshifting and downshifting observed with NMR spectra of C60 and SWCNT adducts to the global and individual ring currents induced in magnetic fields.[2,3]

δ Singlet = 1.93; δ Triplet =1.96; δ Singlet = 2.62; Singlet = 2.75; δ Leaning Pentet = 2.85; δ Leaning Pentet = 3.15; δ Triplet = 3.78; δ Quartet = 4.84; Singlet = 8.47

Assigned Proton Peaks; see [4].

1. Leaning pentets representing neighboring methylenes at the center of the lysine backbone, centered around δ 3.0
2. Amide hydrogen at δ 8.5 (far left side)
3. BOC Signature at δ 1.93
4. Solvent exchangable, diminished pyrrolidine amine at δ 2.75
5. Minute peaks at 7.45 were inconsistently present through repeated analysis and are proposed to represent the partial protonation of the pyrrolidine amine into a cation split by magnetically inequivalent adjacent protons.

**S6Ci**

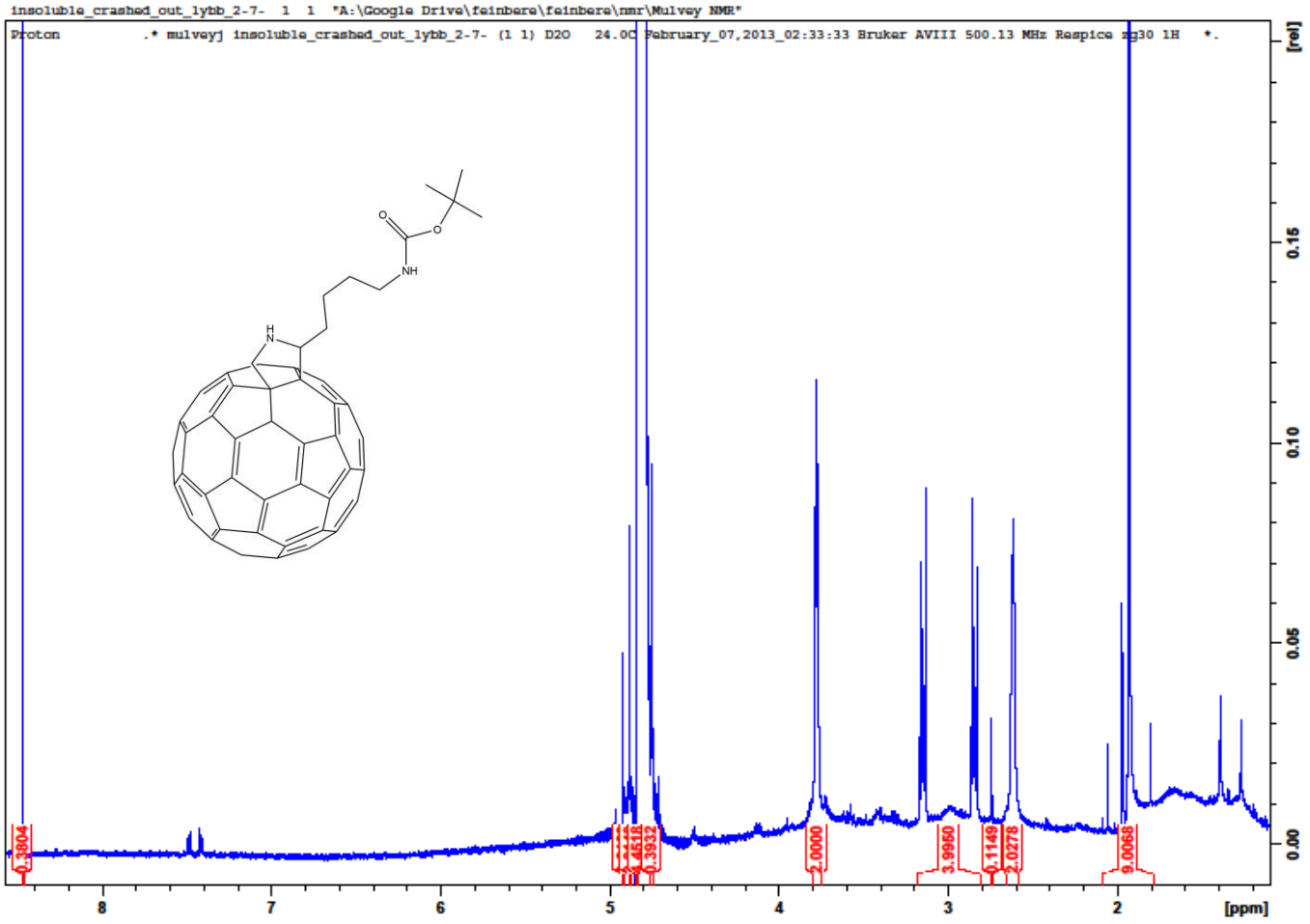

**S6Cii**

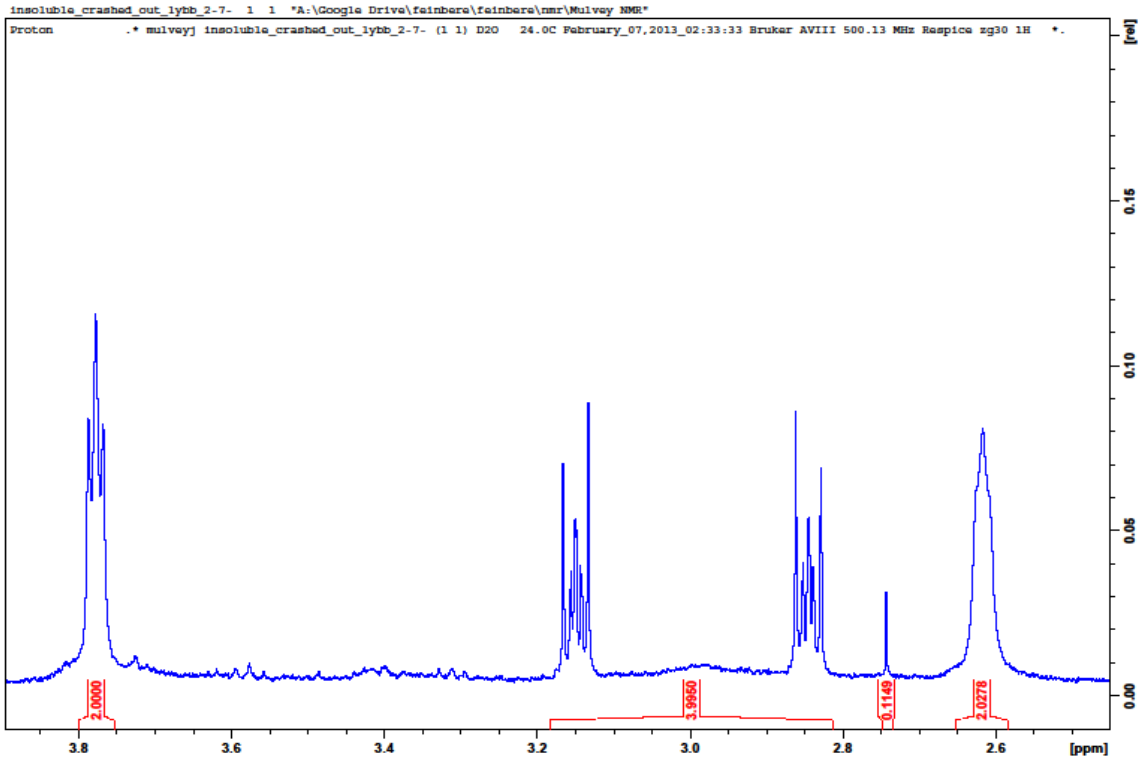


**S6Ciii**

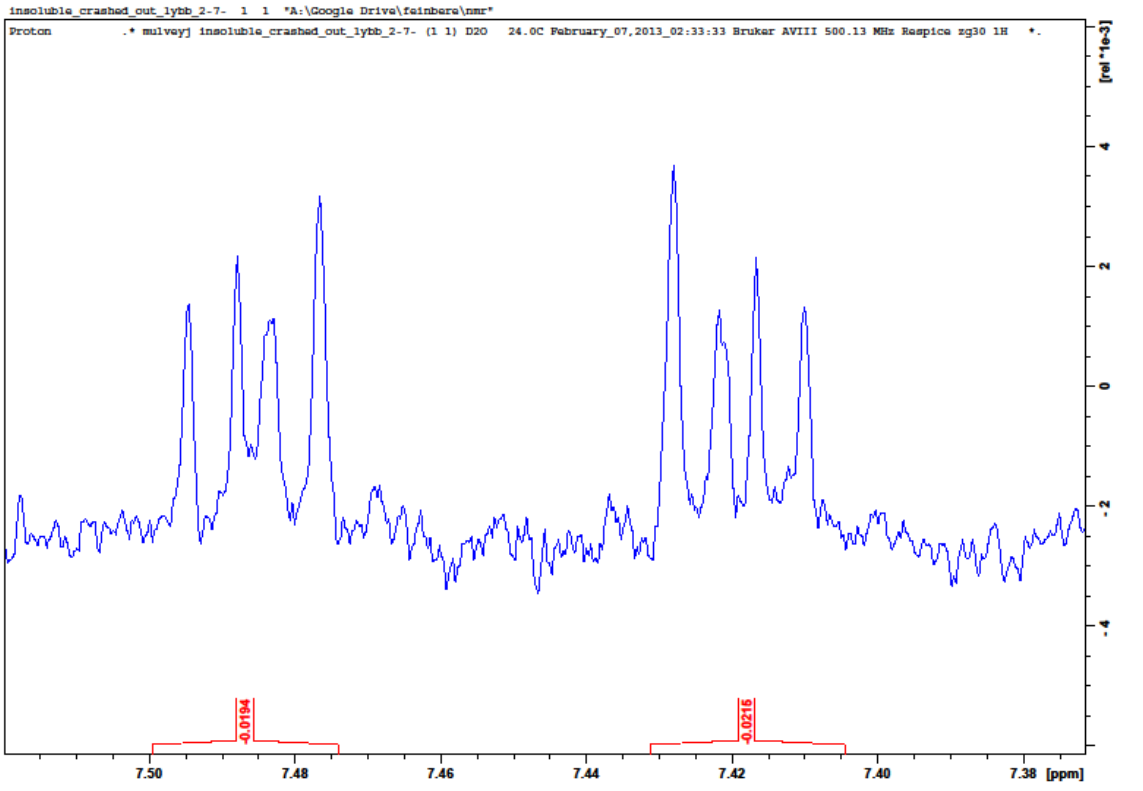

**Figure S6D:** BOC protected Pyrrolidine Adduct on C60 ; Carbon 13 NMR in D2O.

Peak assignments: BOC Carbonyl (177), fullerene peaks (166, 165, 158,157). Quartenary carbon on fullerene (121) Compare to S6b with loss of acid carbonyl (before reaction at 168), the addition of fullerene peaks, and the shifting of adduct chain peaks compared to starting material showing their change in environment due to sphere currents.

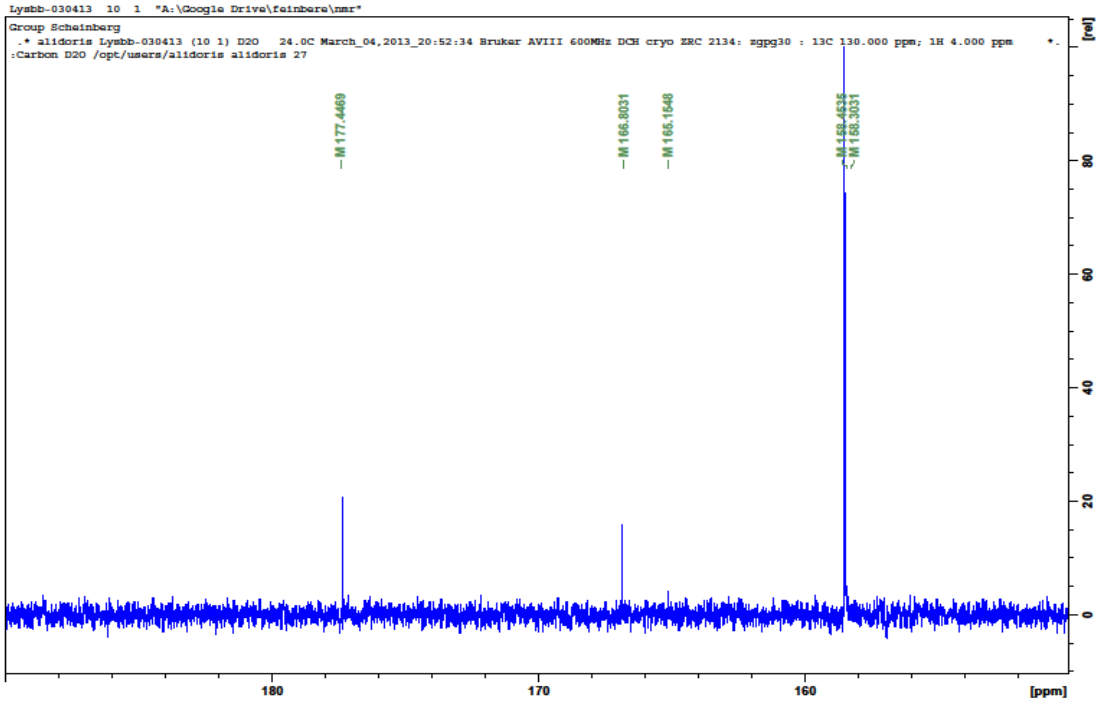


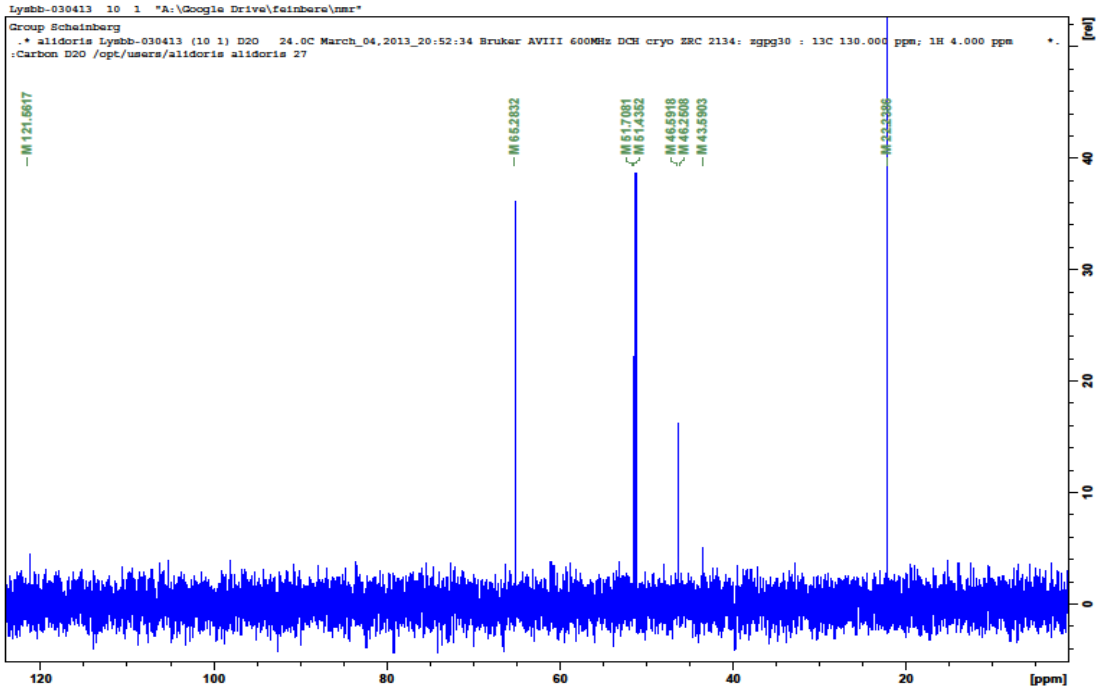

**Figure S7:** Mass Spectroscopy and Calculations for Adducted C60 Molecules

**Figure S7A**: Deprotected Primary Amine Product (3) – 10DG, Dialysis purified, run in MeOH.

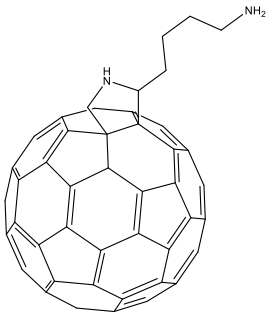


C = 12.011 x 66 = 792.73

N = 14.007 x 2 = 28.014

H = 1.008 x 14 = 14.11

Sum = 834.854

Ionizing proton = 1.008

methanol = 12.011 + 16.000 + 4(1.008) = 32.043

Free Primary Amine

(792.73 + 28.014 + 14.11 + 1.008 + 32.043) = 867.905 (theoretical) Peak found 868.33

(792.73 + 28.014 + 14.11 + 2.016 +64.086)/2 = 450.478 (theoretical) Peak found 448.19

The peak at 668.13 is thought to be an ionization fragment, or very speculatively the double ion of a 5-fold adduct with sodium. (720.66 + 114.19*5 + 23*2)/2 = 668.80 (theoretical) Peak found 668.13

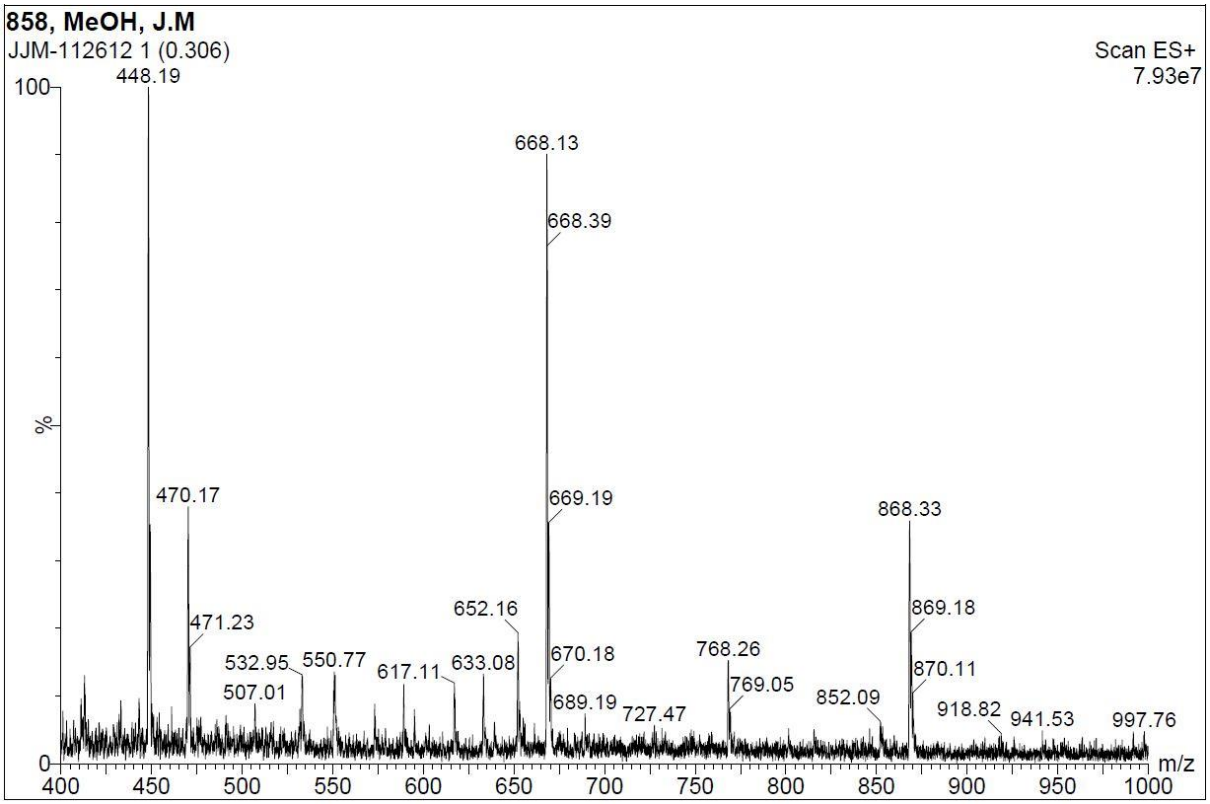

**Figure 7B:** BOC protected Primary Amine Product (4) run in acetonitrile

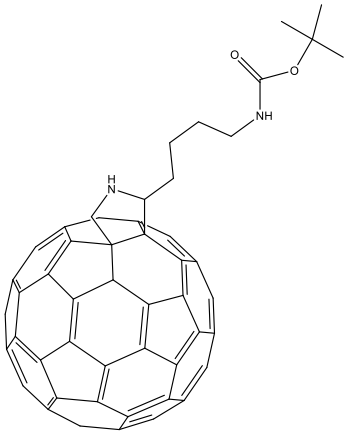


C = 12.011 x 71 = 840.770

N = 14.007 x 2 = 28.014

H = 1.008 x 22 = 22.176

O = 15.999 x 2 = 31.998

Sum = 934.969

Sodium = 23

(934.969 + 23) /2 =  958.977/2 = 478.98 (Theoretical) Peak found 479.11

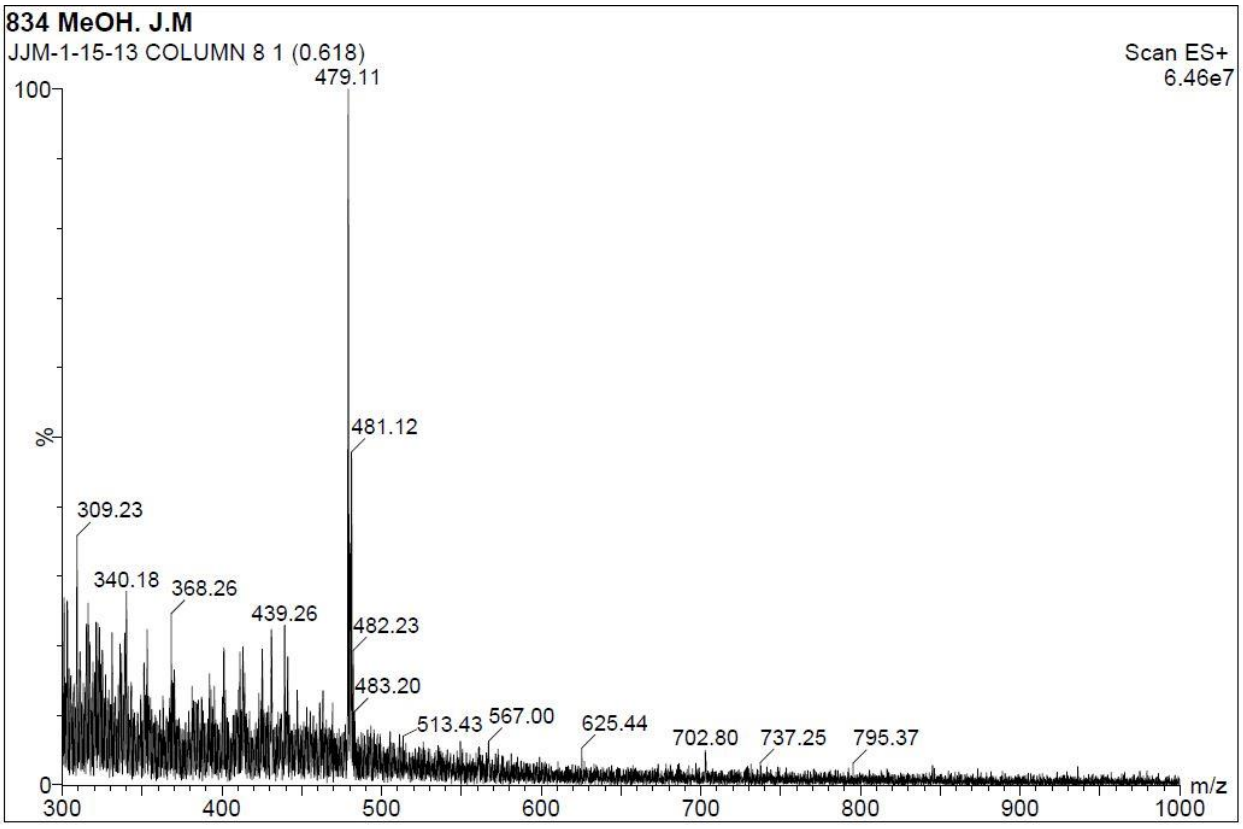

**Figure S8:** Degradation of the modified glycine used in Figure 1a after exposure to room temperature and laboratory light showing PEG fragmentation.

**Figure S8a:** Initial NMR sample taken in DMSO

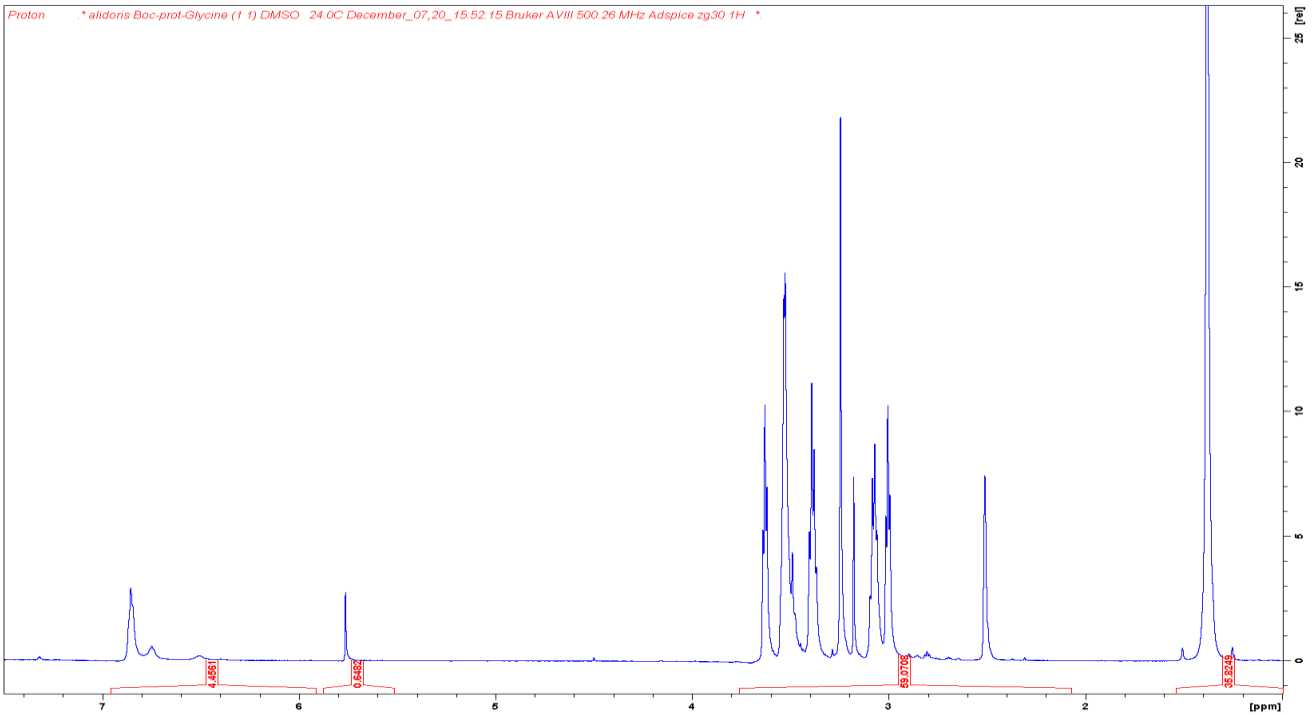


**Figure S8b:** Identical NMR spectrum in DMSO of **S8a** NMR tube contents left at ambient light and temperature for 1 month. Additional peaks, including a broad peak δ4.65 suggestive of PEG decomposition. According to recent literature, this peak is representative of 1,2 Ethanediol in DMSO[5], the bi-product of such fragmentation.

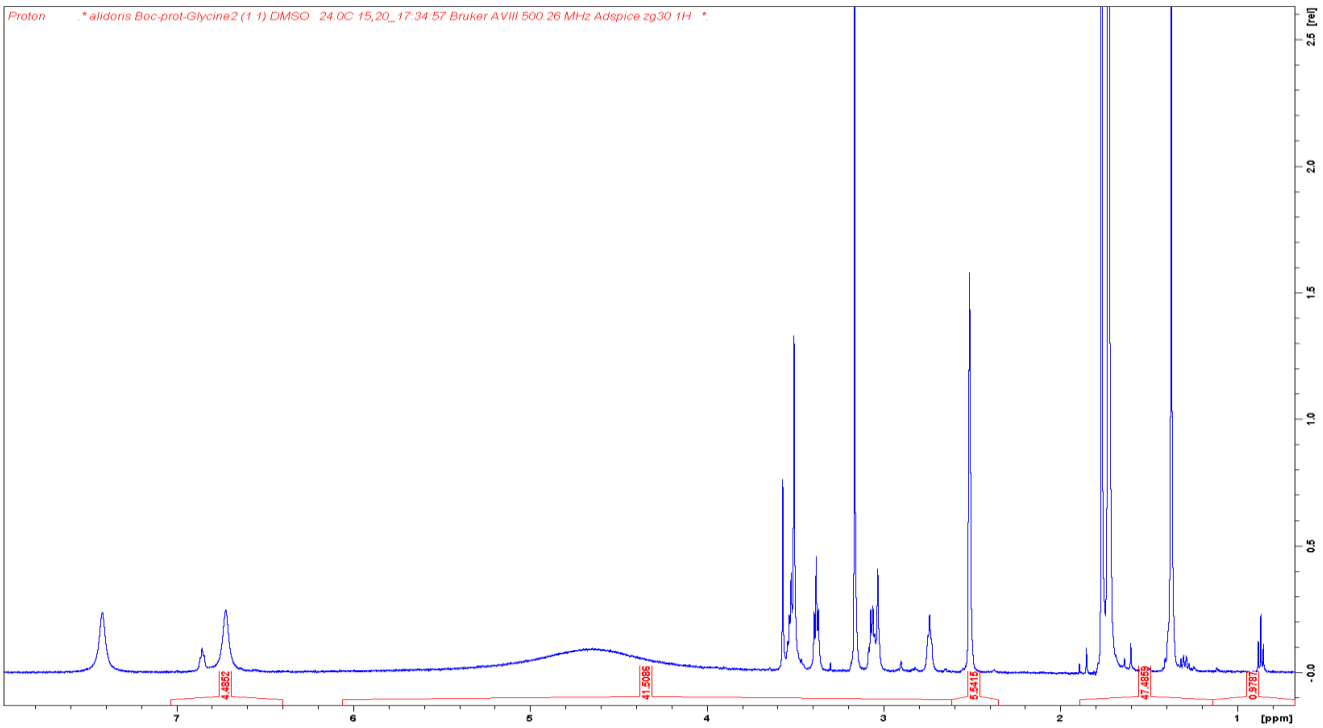

**Figure S9:** RAMAN spectra of: **A)** quartz glass background **B)** stock SWCNTs **C)** BOC-Lysine Modified SWCNTs

Absolute intensity of peaks between spectra varies with different LASER aperture and scan number settings for clearest image and should not be compared. The intensity ratios of peaks of interest to same-spectrum background peaks in the first three spectra provide a basis of allocating intensity to peaks in S9d. For instance, despite their initial presentation, peaks near 1500 $cm^{-1}$ in S9c are at a comparable magnitude to background peaks in S9c indicating that the lysine peaks contribute only scantly to the dband of the modified nanotubes. The area related to the D band is a populous site in this study with weak, broad signals even appearing in background scans. Comparing the "D band" in S9d to background peaks in that spectrum support it to be predominantly a SWCNT-derived D band, with minor contributions from background, and both starting materials. Green dots mark background peaks. There is a reproducible luminescence for plated, water-soluble material (S9c and S9d) between 1000 and 2000 $cm^{-1}$ due to heightened dispersion (ref 31) that has not been altered or removed as baseline.

**A)** Quartz glass Raman spectrum (background)

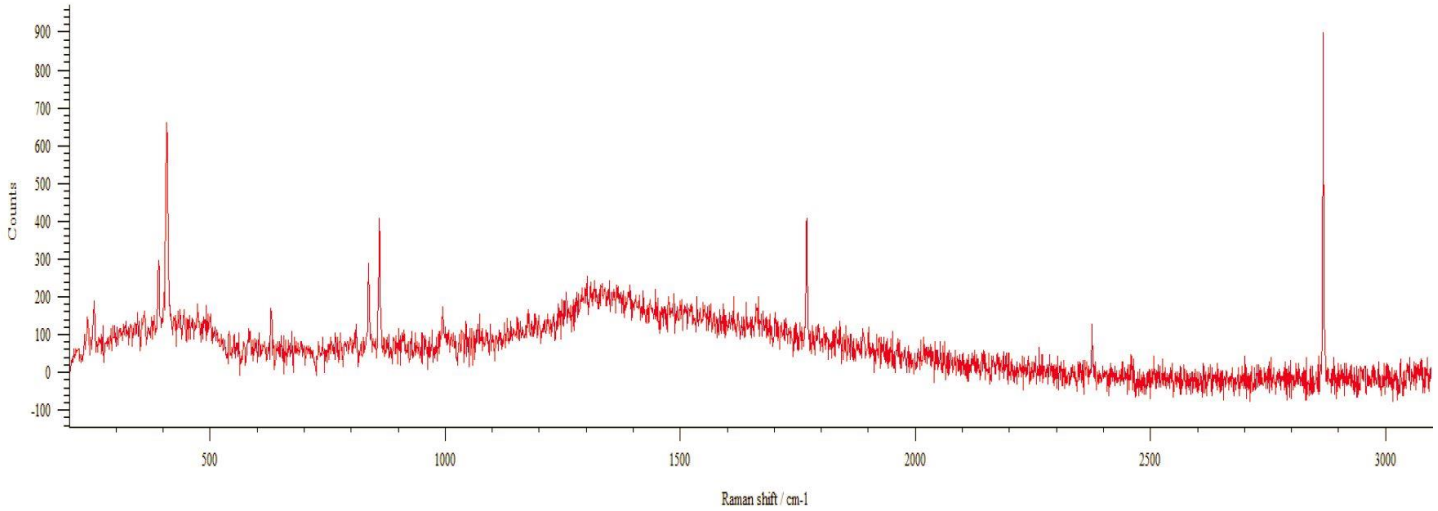


**B)** Stock SWCNTs Raman spectrum. Cosmic Ray (not reproduced) around 980 $cm^{-1}$ was not removed from spectrum. Single peak at ~2880 $cm^{-1}$, two peaks at ~850 $cm^{-1}$, and a single peak at ~410 $cm^{-1}$ represent background peaks.

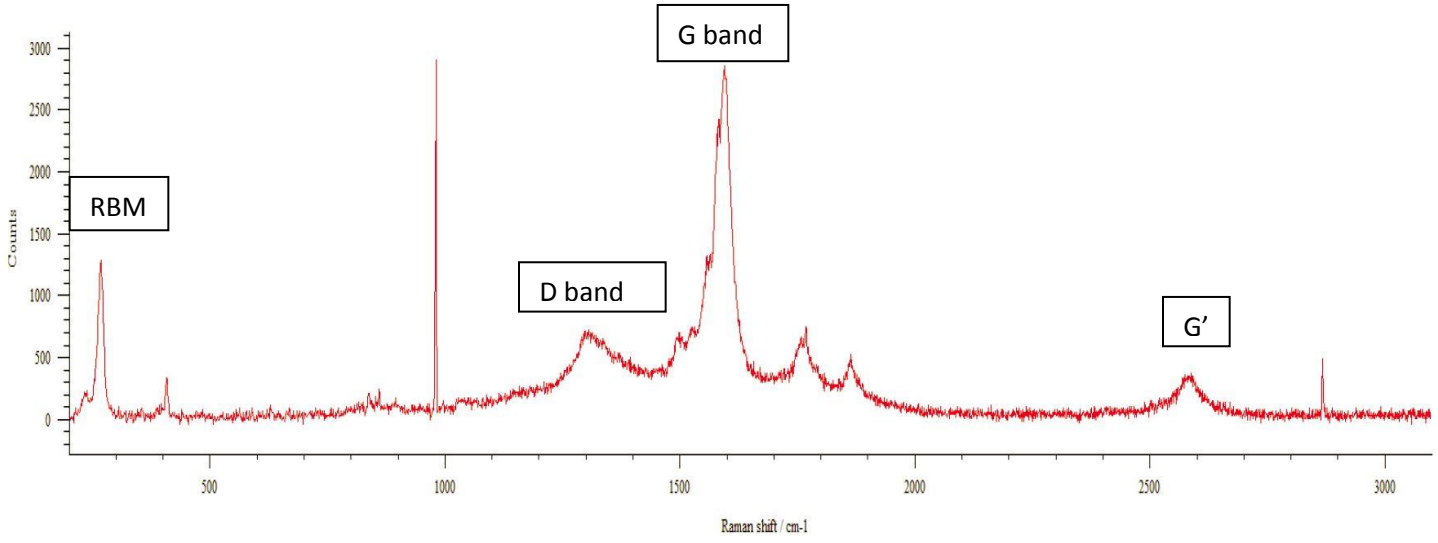

**C)** BOC-Lysine Modified SWCNTs. Single peak at ~2880 $cm^{-1}$, single peak at ~2390 $cm^{-1}$, and a sin G' eak ~410 $cm^{-1}$ represent background peaks. D band presumed enhanced by BOC'd lysine adduct as well as tube modification.

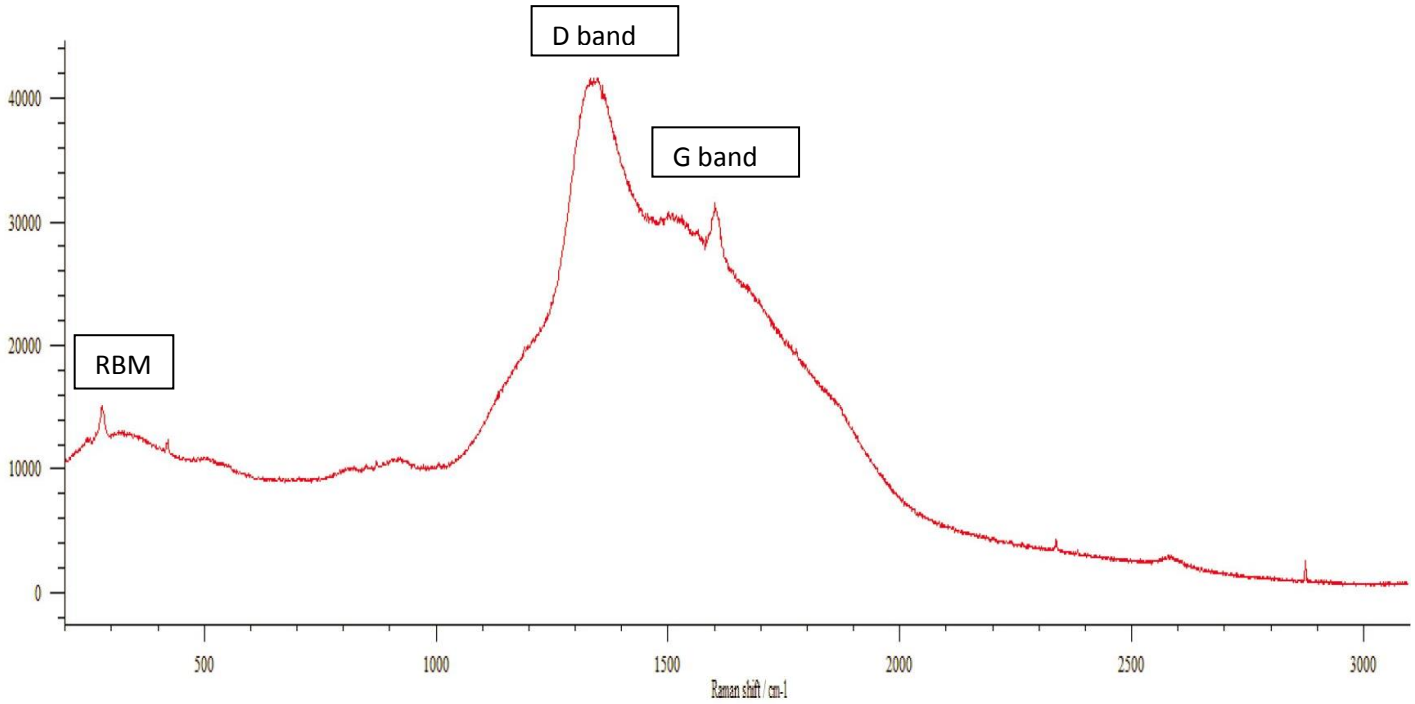


**Figure S10:** HPLC Analysis of SWCNT-Lys-DOTA($^{111}$In),(**5**)

**A)** Urine Alone. (As seen in D and E, some mouse urine peaks are variable)

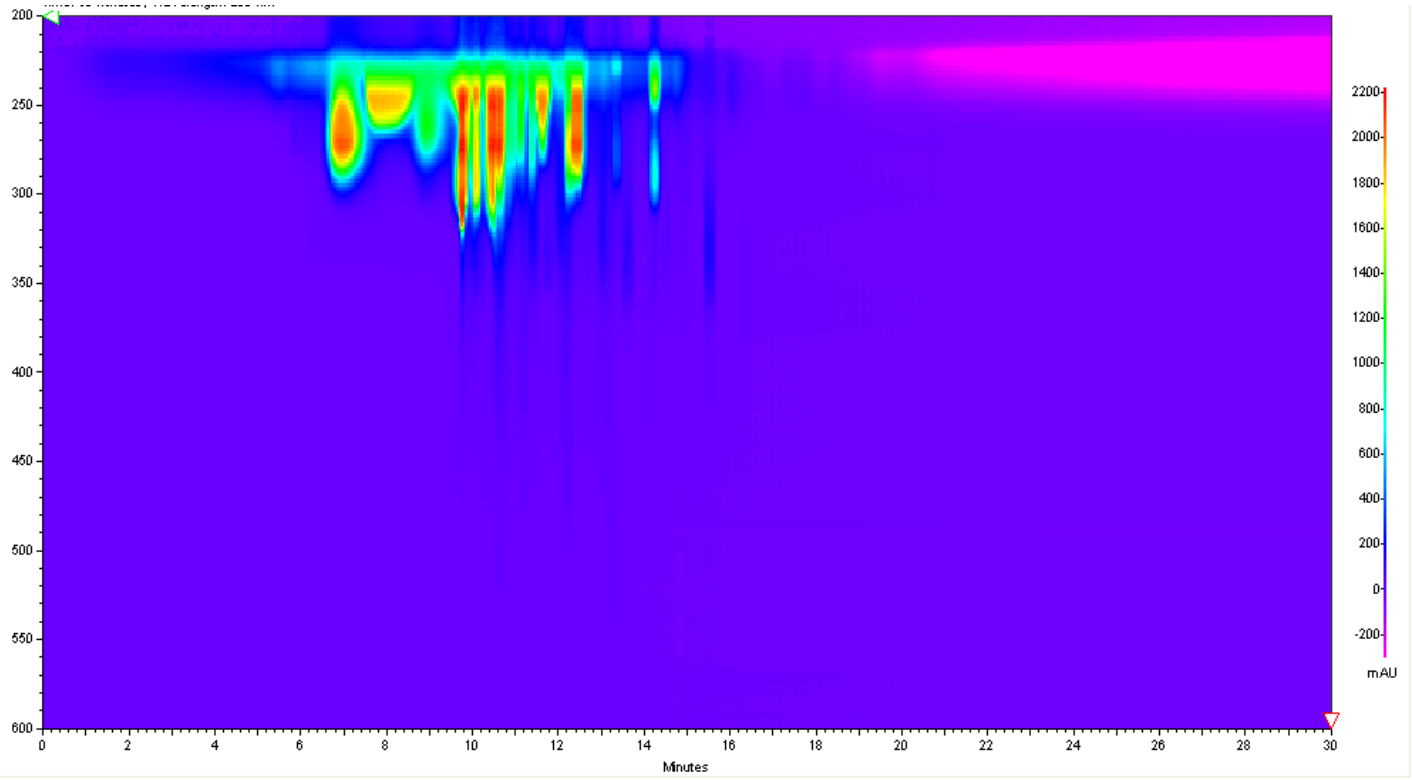

**B)** SWCNT-Lys-DOTA($^{111}$In ), (**5**) after 10DG purification, UV and radio trace of sample  Please note that the radiodectector and UV detector are slightly offset depending on sequence of the HPLC modules

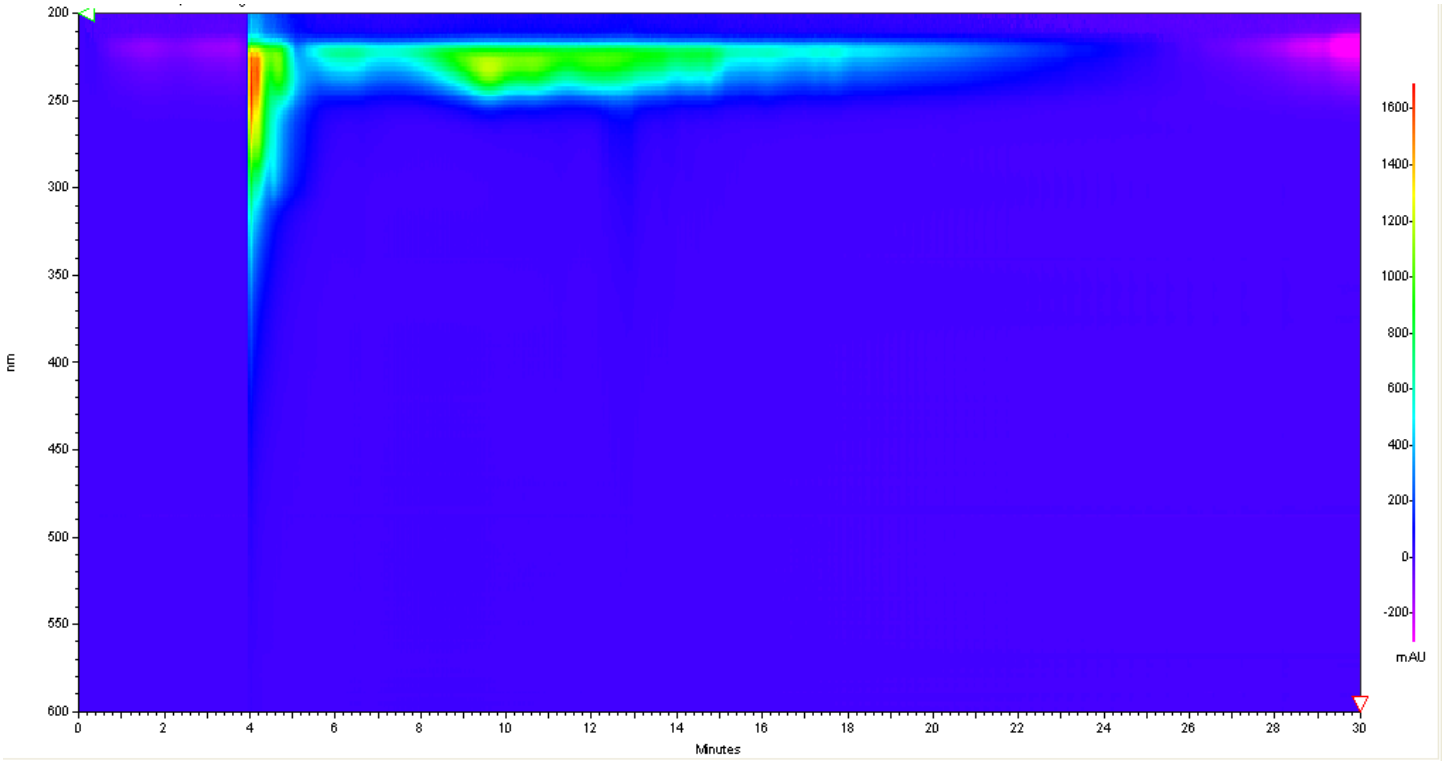


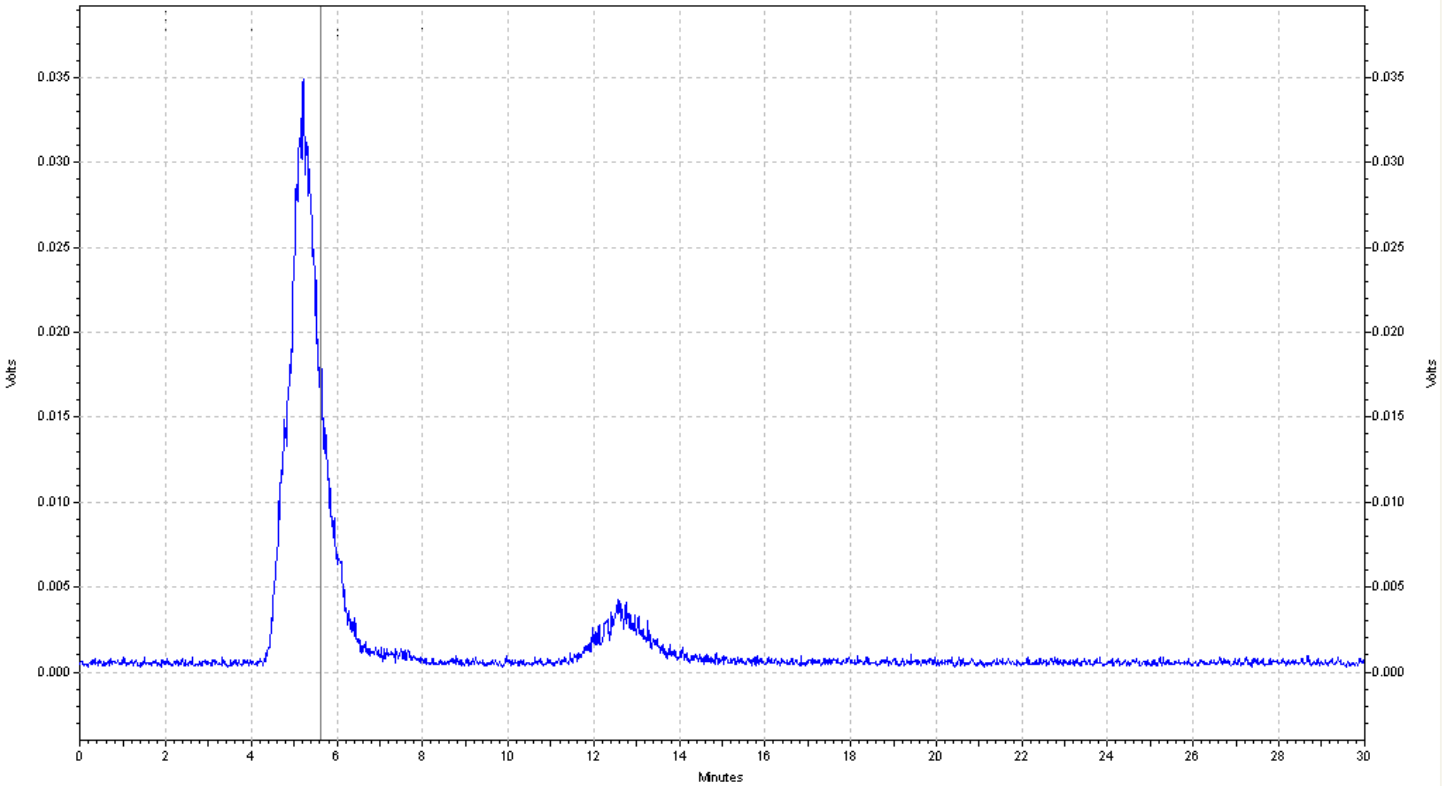

**C)** DOTA-SCN (unattached chelator) alone (multiple peaks represent different SCN group hydrolysis states)

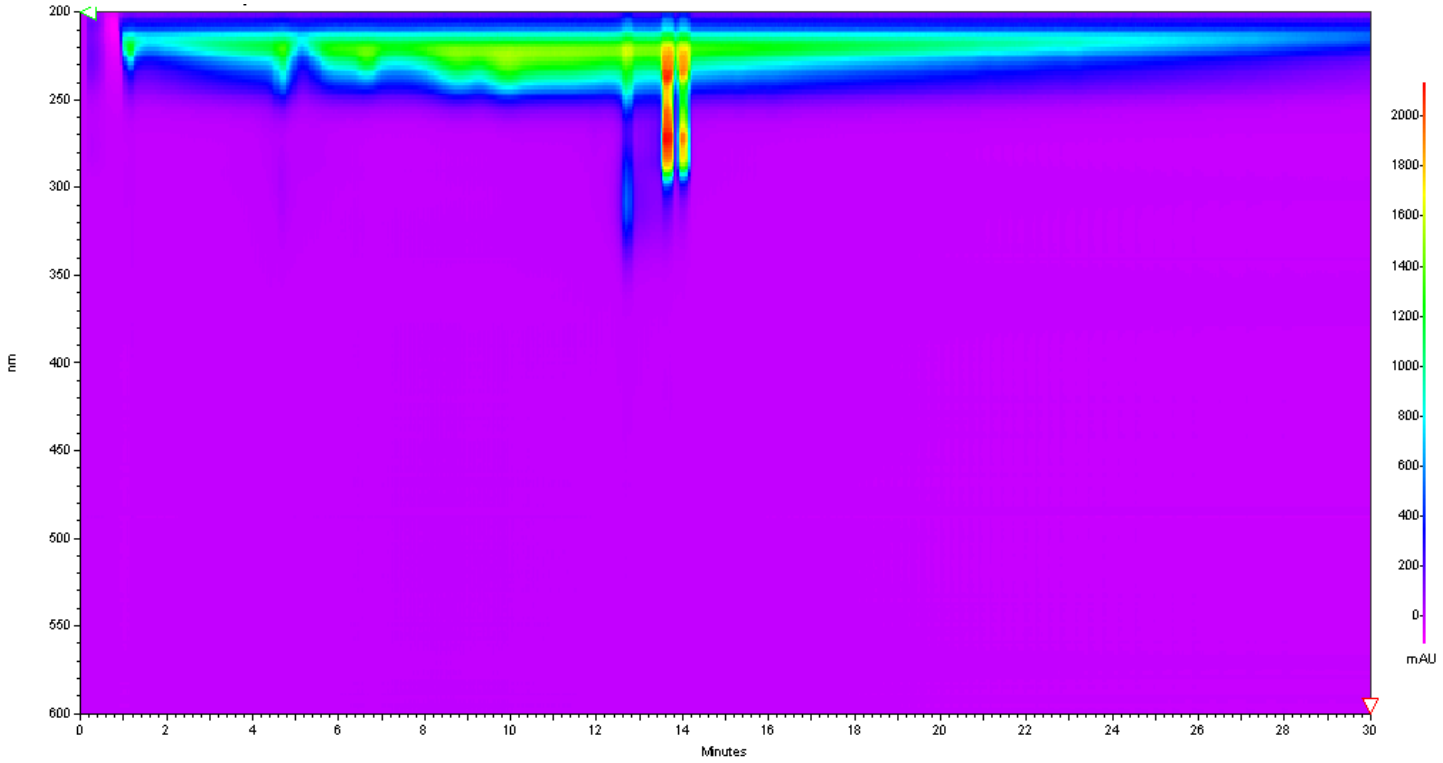


**D)** Unlabelled (**5**) mixed with pre-injection mouse urine

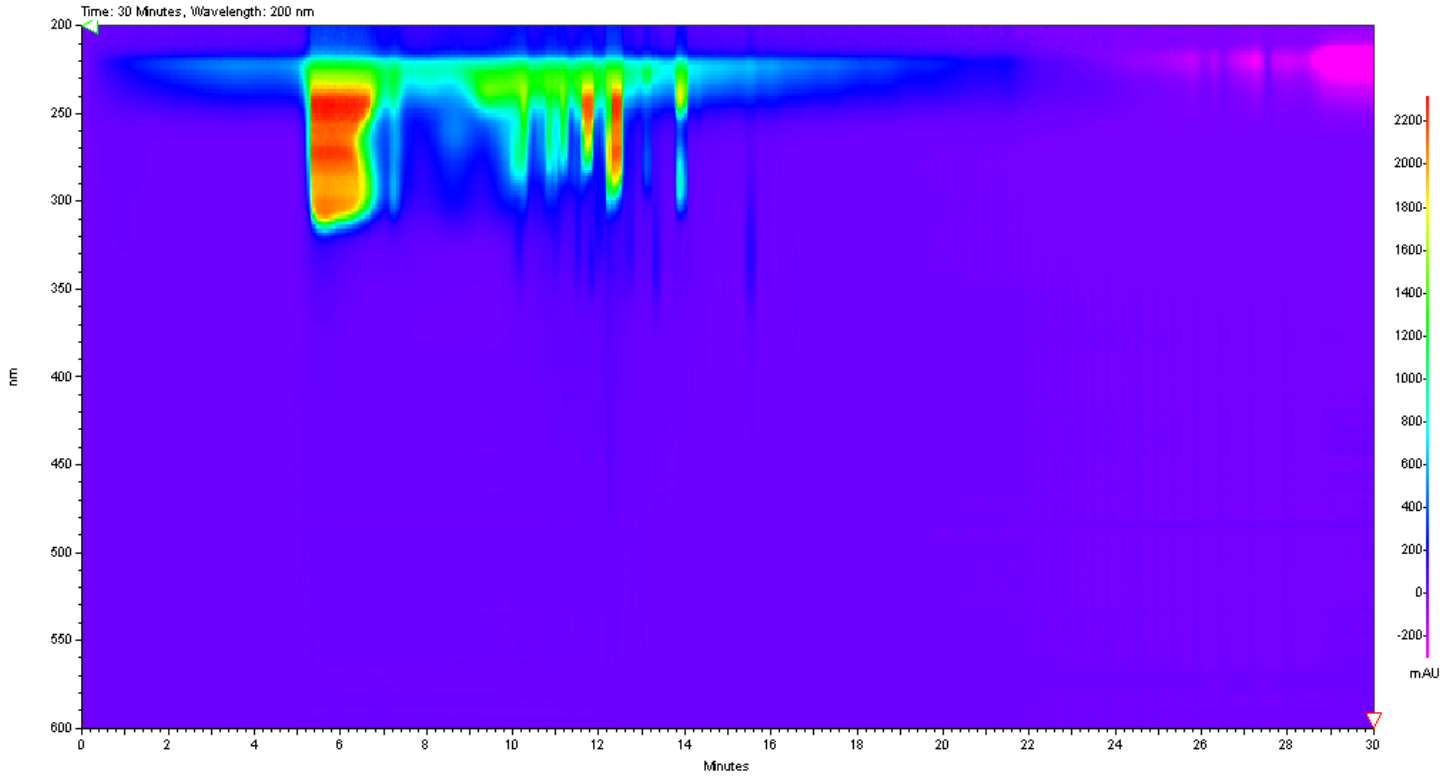

**E)** Vacuum Concentrated mouse IP injected (**5**) collected in urine of the mouse. UV and radio traces. Radioactivity detected after urine vacuum concentration is 33.3 times greater on (**5**) than detached DOTA. This is 97% and representative of the pre-injected radiochemical purity of the sample.

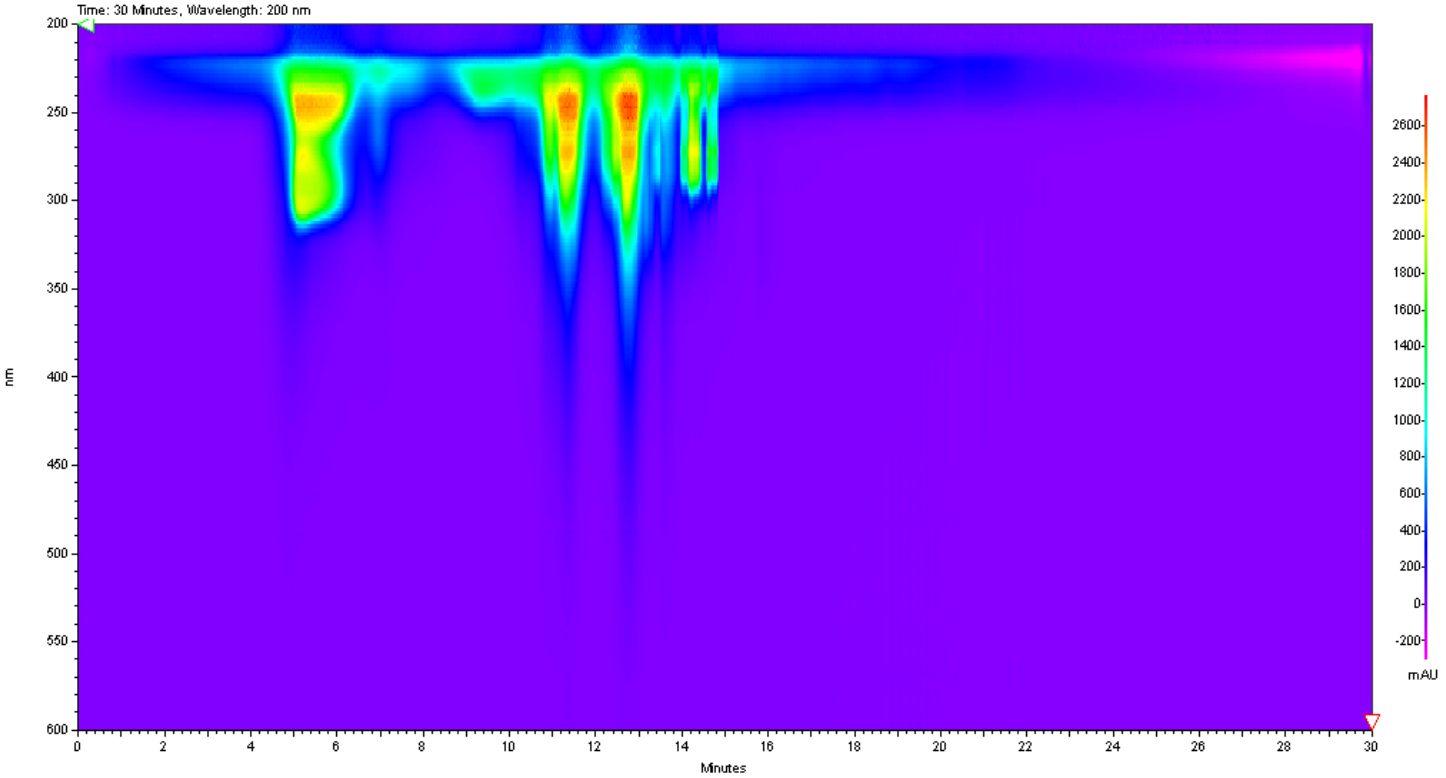


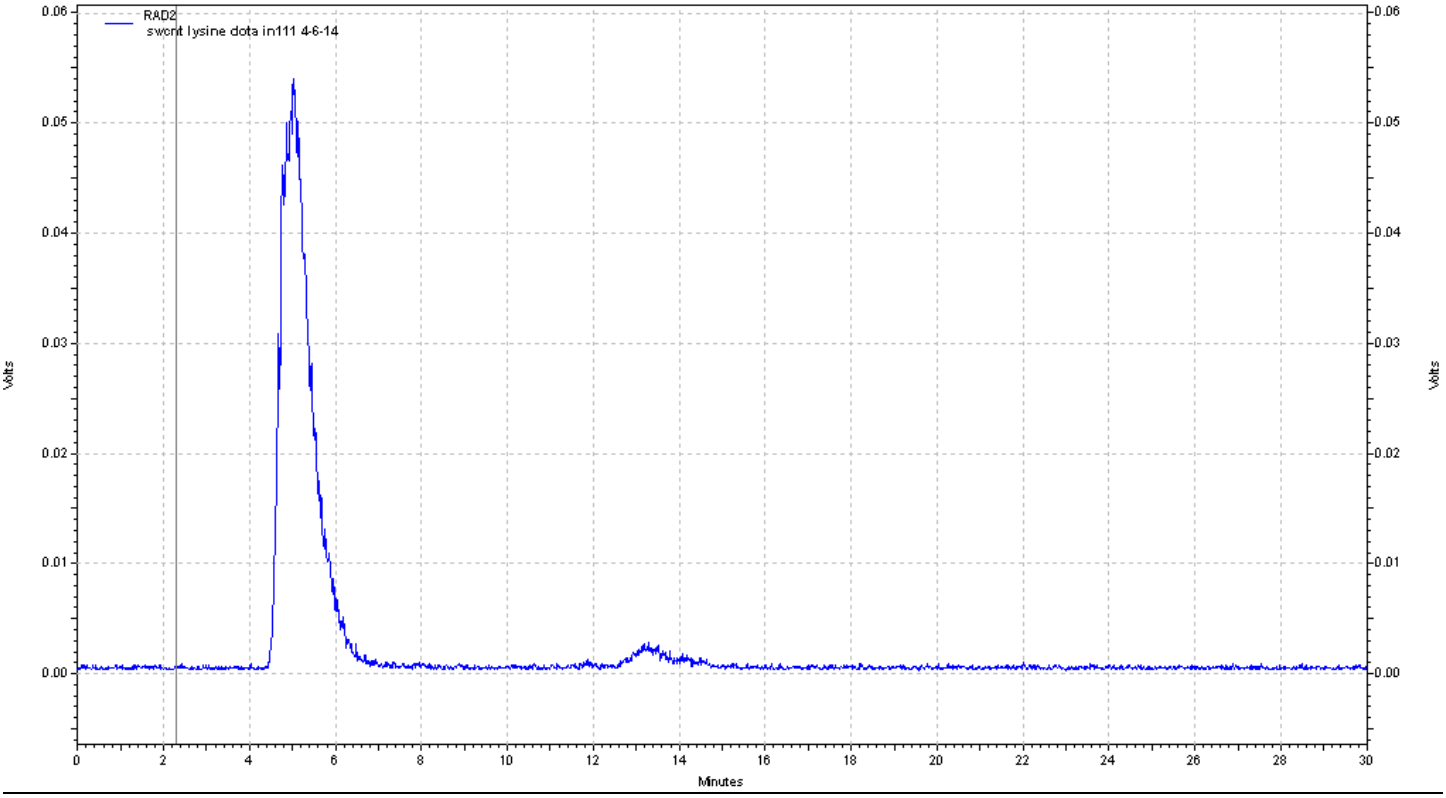

**Supporting Information Literature Cited**


1 K. Sbai, A. Rahmani, H. Chadli, J.-L. Bantignies, P. Hermet, J.-L. Sauvajol, *J. Phys. Chem. B* **2006**, *110*, 12388–12393.

2 M. P. Johansson, J. Jusélius, D. Sundholm, *Angew. Chemie Int. Ed.* **2005**, *44*, 1843–1846.

3 D. Sebastiani, K. N. Kudin, *ACS Nano* **2008**, *2*, 661–668.

4 M. A. Lebedeva, T. W. Chamberlain, M. Schröder, A. N. Khlobystov, *Tetrahedron* **2012**, *68*, 4976–4985.

5 J. S. Lomas, *Magn. Reson. Chem.* **2013**, *51*, 32–41.